

Research Article

Biogenic synthesis of silver nanoparticles *via* indigenous *Anigozanthos manglesii*, (red and green kangaroo paw) leaf extract and its potential antibacterial activity

Monaliben Shah, G errard Eddy Jai Poinern*, Derek Fawcett

Murdoch Applied Nanotechnology Research Group, Department of Physics, Energy Studies and Nanotechnology, School of Engineering and Energy, Murdoch University, Murdoch, Western Australia 6150, Australia

Received: 14 June 2016

Accepted: 02 July 2016

*Correspondence:

Dr. G errard Eddy Jai Poinern,
E-mail: g.poinern@murdoch.edu.au

Copyright:   the author(s), publisher and licensee Medip Academy. This is an open-access article distributed under the terms of the Creative Commons Attribution Non-Commercial License, which permits unrestricted non-commercial use, distribution, and reproduction in any medium, provided the original work is properly cited.

ABSTRACT

Background: Metallic silver nanoparticles with antibacterial properties were biosynthesised for the first time using an indigenous Australian plant *Anigozanthos manglesii*.

Methods: A practical, straight-forward and eco-friendly technique used the *Anigozanthos manglesii* leaf extract, which acted as both reducing and capping agents to create stable silver nanoparticles. The antibacterial activities of the nanoparticles were investigated using the Kirby-Bauer sensitivity method.

Results: Characterisation revealed the nanoparticles ranged in size from 50 nm up to 150 nm, and their morphologies included cubes, triangular plates and hexagonal plates. Antibacterial studies revealed *Deinococcus* was sensitive and susceptible to the biosynthesised nanoparticles. *Escherichia coli* and *Staphylococcus Epidermis* strains were also found to be less susceptible to the silver nanoparticles.

Conclusions: The present study has shown that silver nanoparticles biosynthesised using *Anigozanthos manglesii* leaf extracts have antibacterial activity against *Deinococcus*, *Escherichia coli* and *Staphylococcus Epidermis* bacterial strains

Keywords: Antibacterial, *Anigozanthos manglesii*, Green chemistry, Silver nanoparticles

INTRODUCTION

Over the last decade research in nanotechnology and biological sciences has converged to create the new field of nano-biotechnology. This new multi-disciplined research field combines the principles of green chemistry, biology and nanotechnology to deliver sustainable, eco-friendly and state-of-the-art solutions for a wide range of biomedical, environmental remediation and optoelectronic applications.¹⁻⁸

Much of the research in this field has focused on synthesising metal nanoparticles. Since metals, typically gold (Au) and silver (Ag), at the nanometre scale have unique and distinctive physiochemical properties that are

directly related to their size, size distribution and morphology.⁹ Conventional physical and chemical methods of producing metal nanoparticles have a number of inherent limitations such as cytotoxicity, carcinogenicity and environmental toxicity that result from the use of toxic chemicals and solvents during manufacture.^{10,11}

Understandably, because of toxicity concerns research has focused on developing alternative manufacturing protocols that are clean, non-toxic, and eco-friendly to implement.

However, developing effective eco-friendly methods for producing nanoparticles with a specific size, shape,

composition, desirable surface chemistry and yield still remains a challenge. However, many biological entities offer a viable alternative green chemistry based procedure for producing non-toxic and eco-friendly nanoparticles.^{11,13}

Literature articles have reported the synthesis of a variety of nanoparticles via biological entities such as actinomycetes, bacteria, fungus, plants, viruses and yeast.¹⁴⁻¹⁹ These articles have shown that biological entities can act as factories capable of producing nanoparticles in a nontoxic and eco-friendly manner. Among biological entities, plant-derived extracts offer an eco-friendly source of active biomolecules.

Studies have shown biomolecules present in plant extracts can produce stable metal nanoparticles with a wide range of sizes, shapes, compositions and physicochemical properties.^{20,21} In particular, nanoparticles synthesised via plant extracts are formed much quicker and are generally more stable than those produced by microorganisms.^{22,23}

Anigozanthos manglesii is an indigenous plant found in Western Australia and is more commonly known as the Red and Green Kangaroo Paw. The plant grows annually from an underground rhizome to produce a red stalk that reaches a height of around 1 m as seen in Figure 1 (b). During spring and summer, the stalk is crowned with an array of red and green tubular flowers that open at the apex to form a claw structure that resembles the paw of a kangaroo, hence its name.

This article reports for the first time the synthesis of Ag nanoparticles using a leaf extract derived from the Red and Green Kangaroo Paw plant. The nanoparticles were characterised using UV-visible spectroscopy, transmission electron microscopy (TEM), X-ray diffraction (XRD), scanning electron microscopy (SEM), Fourier transform infrared spectroscopy (FTIR) and energy dispersive spectroscopy (EDS). The report also presents a potential medicinal application via an antibacterial study using the Kirby-Bauer sensitivity method.²⁴ The results of the antibacterial study revealed that *Deinococcus* was sensitive and susceptible, while both *Escherichia coli* and *Staphylococcus Epidermis* were resistant to the synthesised Ag nanoparticles.

METHODS

The source of Ag⁺ ions came from analytic grade silver nitrate [AgNO₃, (99.99%)] supplied by Sigma-Aldrich (Castle Hill, NSW, Australia) and was used as supplied. The Milli-Q[®] water (MQ water) used to make all aqueous solutions was produced by a Ultrapure Water System (D11931 Barnstead, 18.3 MΩ cm⁻¹) supplied by Thermo Scientific. Healthy *Anigozanthos manglesii* leaves were randomly selected from several plants (Figure 1) located at various sites around the Murdoch University campus. The leaves were thoroughly washed in MQ water before

being processed in a standard domestic blender. After blending 50 mL's of MQ water was slowly added to the blend under the influence of slow stirring. The blend was then homogenised at 5000 rpm for 10 min at room temperature (24°C) using a IKA[®] T25 Digital Ultra-Turrax[®] Homogeniser.

After homogenization initial filtration was carried out using a Hirsch funnel to remove leaf debris. This was followed by two further filtrations using two separate 0.22 μm Millex[®] (33 mm Dia.) syringe filters. The processed leaf extract was then stored in glass vials ready for use.

Ag nanoparticle synthesis

The influence of varying concentrations of leaf extract on Ag nanoparticle synthesis at room temperature (24 °C) was investigated by adjusting the amount of leaf extract (1 mL for s1, 2 mL for s2 and 3 mL for s3). The procedure involved a fixed amount of processed leaf extract being mixed via stirring with a 1.0 mL solution of 0.1M AgNO₃ for 1 minute.

After combining the mixture was allowed to stand while silver reduction took place. Control nanoparticles were formed by first stirring a 1.0 mL solution of 1 mM AgNO₃ to a 10 mL solution of MQ water. This was followed by adding a 1.0 mL solution of 1mM sodium citrate (stabilizing and capping agent) while stirring. Reduction of Ag nanoparticles was initiated by stirring a 1.0 mL solution of 0.01 M sodium borohydride to the mixture at room temperature (24°C).

Advanced characterisation

UV-visible spectroscopy (Varian Cary 50 series UV-Visible spectrophotometer V3) was used to monitor nanoparticle formation and record the maximum surface plasma resonance over the 200 to 800 nm spectral range. The crystalline structure of the synthesised Ag nanoparticles were examined using a Bruker D8 series diffractometer with flat plane geometry operating at 40 kV and 30 mA [Cu Kα = 1.5406 Å radiation source]. While the diffraction pattern was collected over a 2θ range starting at 15° and finishing at 80°.

A JEOL JCM-6000, NeoScopeTM scanning electron microscope (SEM) was used to ascertain particle size and morphology. The energy dispersive spectroscopy (EDS) attachment was used to identify the presence of Ag and other elements in the samples. All samples were mounted on holders using carbon adhesive tape before being coated with a 2 nm layer of gold via a sputter coater (Cressington 208HR) to prevent charge build up.

For transmission electron microscopy (TEM), a single sample drop was pipetted onto a carbon-coated grid and then allowed to dry at room temperature. Micrographs were taken using a Phillips CM-100 electron microscope

(Phillips Corporation Eindhoven, The Netherlands) operating at 80kV. The major functional groups and vibration modes of the samples were determined by a Perkin-Elmer Frontier FT-IR spectrometer fitted with a universal single bounce diamond (ATR) attachment.

Antibacterial assay

The antibacterial activity of the synthesised Ag nanoparticles was investigated using the sensitivity method of Kirby-Bauer.²⁴ Bacteria used in the antibacterial challenge were *Deinococcus*, *Escherichia coli* and *Staphylococcus Epidermis*. The sub-cultured bacteria were swabbed uniformly over nutrient agar medium coated Petri dishes (Dia. 90) using a sterile cotton swab. Then 50 µL nanoparticle sample solutions were deposited on sterile disks (6 mm Whatman® AA 2017-006) using a micropipette. The disks were then allowed to air dry for 20 minutes before being placed on the respective bacteria treated agar plates using sterile forceps. The plates were then incubated at 37 °C for 48 h. Following incubation, the zone of inhibition of the various bacterial strains was measured, compared and the antibacterial performance of the Ag nanoparticles appraised.

RESULTS

A Biogenic synthesis of Ag nanoparticles occurred within 20 minutes, with the results of the reaction clearly visible. Initially, the pale green coloured mixture containing leaf extract and AgNO₃ progressively turned dark brown as seen in a representative sample s2 in Figure 1 (a) insert. Figure 1 (a) also presents a representative UV-Visible spectra for an s2 sample showing an optical Surface Plasmon Resonance (SPR) peak at 435 nm. Studies reported in the literature indicate the resulting brown colour is typical and shows the formation of metallic Ag nanoparticles (Figure 1).^{13,14}

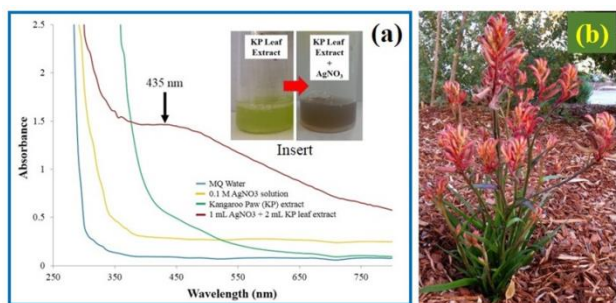


Figure 1 (a) UV-visible spectrophotometer analysis of Ag nanoparticles; insert shows colour change induced by the reduction and stabilisation of Ag nanoparticles and (b) *Anigozanthos manglesii* (red and green kangaroo paw) plant specimen at murdoch university campus.

TEM examination of the samples reveals the presence of Ag nanoparticles with different sizes and shapes as seen

in Figures 2 (a) and 2 (b). Further characterisation via XRD revealed the crystalline nature of the Ag nanoparticles. Representative results are presented in Figure 2 (c) and reveal a dominant (111) Bragg reflection peak consistent with similar reports for biologically synthesised Ag nanoparticles (Figure 2).^{26,27}

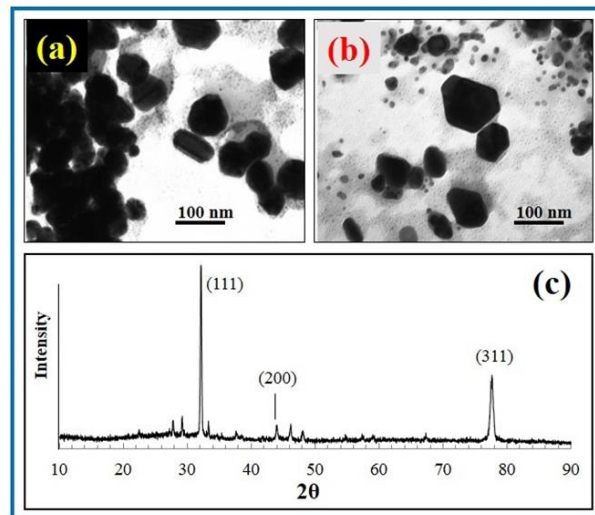


Figure 2 (a) and (b) representative high-resolution TEM images of reduced Ag nanoparticles and (c) XRD analysis of a typical sample containing Ag nanoparticles showing the crystalline phases present.

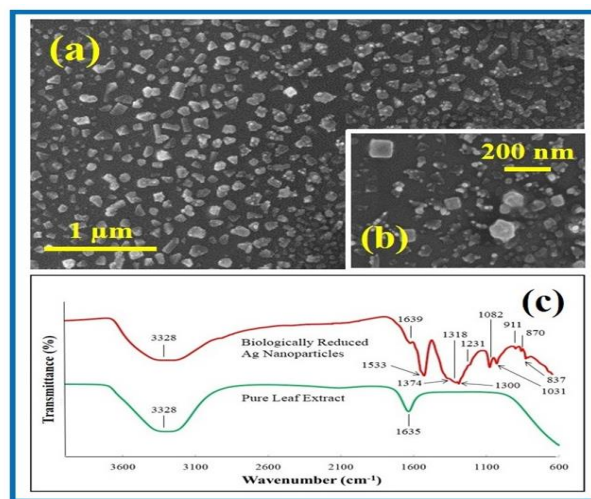


Figure 3 (a) Representative SEM micrograph showing an array of various sized Ag nanoparticles, insert (b) showing higher magnification image highlighting the various polygonal nanoparticle shapes present and (c) FT-IR spectroscopy analysis of representative samples of a pure leaf extract sample and a leaf extract/AgNO₃ reaction mixture.

The FT-IR spectra of pure leaf extract and bio-reduced Ag nanoparticles from leaf extract and AgNO₃ are presented in Figure 3 (c). The pure leaf extract consists of only two adsorption bands located at 1635 and 3328

cm^{-1} , while the leaf broth mixture contained a further seven adsorption bands located at 1031, 1082, 1231, 1318, 1374, 1533 and 1639 cm^{-1} (Figure 3).

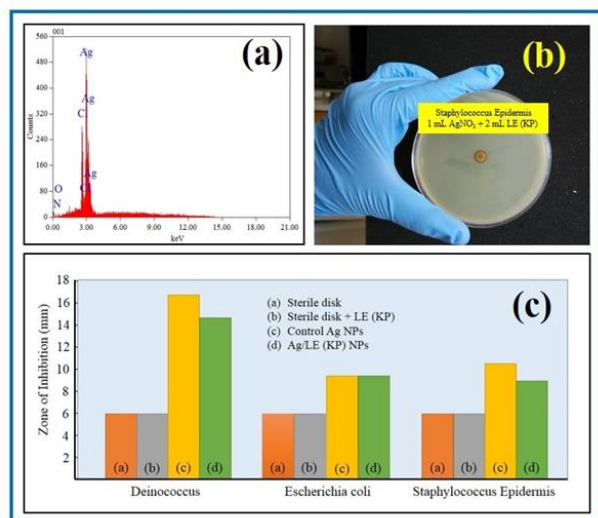


Figure 4 (a)EDS elemental analysis showing the strong presence of metallic Ag, (b) A representative petri dish sample of *Staphylococcus epidermis* being challenged by leaf extract mediated Ag nanoparticles and (c) Graphical Summary of antibacterial challenge test results for the three bacterial strains.

Potential antibacterial properties of Ag nanoparticles were studied using the sensitivity method of Kirby-Bauer. The results of the antimicrobial study revealed a null result for the leaf extract. But, the biologically synthesised Ag nanoparticles when challenged by the three bacterial strains produced zones of inhibition, which were measured. *Deinococcus* recorded a mean inhibition zone of 14 mm, *Escherichia coli* a mean value of 9 mm and *Staphylococcus Epidermis* a mean value of 8 mm. A typical antibacterial test petri dish is presented in Figure 4 (b) and representative results of the antibacterial challenge are summarised and presented graphically in Figure 4 (c) (Figure 4).

DISCUSSION

Biogenic synthesis of Ag nanoparticles turned the reaction fluid dark brown in colour and produced a (SPR) peak at 435 nm. Studies in the literature have reported modelling based on Mie's theory of the absorption spectra tends to produce a single intense SPR peak for spherical metal nanoparticles. The broad peak located at 435 nm seen in absorption spectra presented in Figure 1 (a) suggests the synthesised Ag nanoparticles have an anisotropic nature.

The anisotropic nature was confirmed by TEM images that revealed the presence of nanoparticles with different sizes and shapes. Figures 2 (a) and 2 (b) presented representative micrographs taken after a 20 minute

synthesis period. Examination of the images revealed the nanoparticles ranged in size from 50 nm up to around 150 nm. The shapes seen in the micrographs included cubes, triangular plates and hexagonal plates.

Figure 2 (c) presents a representative XRD pattern of a dried sample and reveals the presence of a dominant peak that corresponds to the (111) Bragg reflection for Ag. Also present in the pattern is two smaller peaks corresponding to the (200) and (311) Bragg reflections for Ag. The presence of these peaks in the samples indicates a face centred cubic structure was present in the formed Ag nanoparticles and the occurrence of peak broadening supports nanoparticle formation.

The XRD results were found to be consistent with nanoparticle seen in TEM micrographs presented in Figure 2 and are consistent with similar reports for biologically synthesised Ag nanoparticles.^{26,27} Furthermore, a much larger landscape SEM image of synthesised Ag nanoparticles presented in Figure 3 (a) and corroborates the presence cubic, triangular and hexagonal shaped particles seen in the TEM micrographs. The enlarged SEM image presented in Figure 3 (b) confirms that the biologically synthesised nanoparticles are smaller than 200 nm, with many of them smaller than 100 nm.

Analysis of the FT-IR spectra revealed that the 1031, 1318, and 1639 cm^{-1} bands were characteristically associated with the biological reduction of Ag ions. The strong and broad band located at 3328 cm^{-1} in the samples results from bounded hydroxyl (-OH) or amine (-NH) groups present in the bio-macromolecules in the leaf extract. The weak band located at 1639 cm^{-1} and the much stronger band located at 1533 cm^{-1} indicates the presence of amide I and amide II, and arise from carbonyl stretching and -N-H stretching vibrations respectively. While the adsorption band located at 1318 cm^{-1} corresponds to C=C stretching of aromatic amines. As a final characterisation, EDS analysis confirmed the formation of Ag nanoparticles in the leaf broth mixture as seen in Figure 4 (a) by the presence of a strong elemental signal for Ag.

Potential antibacterial properties of Ag nanoparticles chemically (control) and leaf extract mediated synthesis were tested against *Deinococcus*, *Escherichia coli* and *Staphylococcus Epidermis*. The Petri dishes containing cultured bacteria samples and untreated sterile pads were first studied to establish a baseline for zone of inhibition measurements.

This was followed by examining the antibacterial effect of sterile pads treated with pure leaf extract. The investigation found pure leaf extract treated disks were the same as the untreated disks. The null result indicated the leaf extract had no antibacterial effect against *Deinococcus*, *Escherichia coli* and *Staphylococcus Epidermis*. Next, petri dishes, each containing a single

sterile pad treated with chemically synthesised Ag nanoparticles (control) were challenged by each respective bacterial strain and each zone of inhibition was recorded.

The challenge recorded a zone of inhibition of 16 mm for *Deinococcus*, 9 mm for *Escherichia coli* and 10 mm for *Staphylococcus Epidermis*. Finally, biologically synthesised Ag nanoparticles were challenged by the respective bacterial strains and zones of inhibition were measured. *Deinococcus* recorded a mean inhibition zone of 14 mm, *Escherichia coli* a mean value of 9 mm and *Staphylococcus Epidermis* a mean value of 8 mm. A representative antibacterial test petri dish is presented in Figure 4 (b) and the results of the antibacterial challenge are summarised and presented graphically in Figure 4 (c).

Inspection of Figure 4 (c) reveals the zones of inhibition for all disks treated with Ag nanoparticles produced via leaf extract tend to be slightly smaller or equal to the control treatment. *Deinococcus* was found to be sensitive and susceptible to Ag nanoparticles produced by both synthesis routes. While both *Escherichia coli* and *Staphylococcus Epidermis* were found to be resistant to Ag nanoparticles produced by both synthesis routes.

Differences in the size of the zones of inhibition between the two Ag nanoparticle treatments is believed to result from surface attachment of biomolecules present in the leaf extract. During biological synthesis, biomolecules present in the leaf extract act initially to reduce the AgNO₃ to form metallic Ag nanoparticles. Following formation, other biomolecules present in the leaf extract act as a capping agent to stabilise the nanoparticles and prevent particle agglomeration. The presence of biomolecules coating the surface of Ag nanoparticles appears to moderate their antibacterial properties and reduce their effectiveness against the bacterial strains studied as seen in Figure 4 (c).

The types of biomolecules involved in first reducing and then capping the formed Ag nanoparticles is currently under investigation. Also currently under investigation is the influence of capping biomolecules, coating structure on Ag nanoparticles and their interaction with microorganisms. The results of these studies will be published in a future article.

CONCLUSION

The present work has shown that a leaf extract taken from *Anigozanthos manglesii* (Red and Green Kangaroo Paw) was capable of synthesising stable Ag nanoparticles. The room temperature and eco-friendly process followed the principles of green chemistry. Nanoparticles ranged in size from 50 nm up to around 150 nm and produced cubic, triangular and hexagonal plate morphologies.

While UV-Visible spectroscopy revealed a SPR peak at 435 nm and EDS analysis confirmed the presence of a

strong elemental signal for Ag in the samples. Subsequent XRD pattern analysis indicated a face centred cubic structure was present in the formed Ag nanoparticles and peak broadening confirmed nanoparticle formation.

The room temperature synthesis process confirmed that biomolecules present in the leaf extract acted as both reducing agent and stabilising agent. Antibacterial studies using the sensitivity method of Kirby-Bauer revealed that *Deinococcus* was sensitive, while both *Escherichia coli* and *Staphylococcus Epidermis* were found to be resistant to the synthesised Ag nanoparticles.

However, further studies are needed to confirm the medicinal properties of the leaf extract mediated Ag nanoparticles, the influence of biomolecules in forming the nanoparticles and their subsequent interaction with various microorganisms.

ACKNOWLEDGEMENTS

Authors would like to acknowledge Murdoch University for providing her PhD Scholarship to undertake her PhD project. This work was partly supported by Horticulture Innovation Australia Project A114003 and Derek Fawcett would like to thank Horticulture Innovation Australia for their research fellowship. The authors would also like to thank Mr Ravi Krishna Brundavanam for his assistance with the XRD measurements.

Funding: Horticulture innovation Australia project A114003

Conflict of interest: None declared

Ethical approval: Not required

REFERENCES

1. Parak WJ, Gerion D, Pellegrino T, Zanchet D, Micheel C, Williams SC, et al. Biological Applications of Colloidal Nanocrystals. *Nanotechnology*. 2003;14(7):15-27.
2. Sperling RA, Gil PR, Zhang F, Zanella M, Parak WJ. Biological applications of gold nanoparticles. *Chem. Soc. Rev.* 2008;37:1896-908.
3. Cai W, Gao T, Hong H, Sun J. Applications of gold nanoparticles in cancer nanotechnology. *Nanotechnology, Science and Applications*. 2008;1:17-32.
4. Barakat MA. New trends in removing heavy metals from industrial wastewater. *Arabian Journal of Chemistry*. 2001;4:361-77.
5. Smith AM, Duan H, Rhyner MN, Ruan G, Nie S. A Systematic Examination of Surface Coatings on the Optical and Chemical Properties of Semiconductor Quantum Dots. *Physical Chemistry Chemical Physics*. 2006;8(33):3895-903.
6. Alshehri AH, Jakubowska M, Młozniak A, Horaczek M, Rudka D, Free C, et al. Enhanced Electrical Conductivity of Silver Nanoparticles for

- High Frequency Electronic Applications. ACS Appl. Mater. Interfaces. 2012;4(12):7007-10.
7. Salata OV. Applications of nanoparticles in biology and medicine. Journal of Nanobiotechnology. 2004;2(3):1-6.
 8. Zaniewski AM, Schriver M, Lee JG, Crommie MF, Zettl A. Electronic and optical of metal nanoparticles filled graphene sandwiches. J. Appl. Phys. Lett. 2013;102:023108,1-5.
 9. Le X, Poinern GEJ, Subramaniam S, Fawcett, D. Applications of Nanometre Scale Particles as Pharmaceutical Delivery Vehicles in Medicine. Open Journal of Biomedical Materials Research. 2015;2(2):11-26.
 10. Ai J, Biazar E, Jafarpour M, Montazeri M, Majdi A, Aminifard S, et al. Nanotoxicology and nanoparticle safety in biomedical designs. Int. J. Nanomedicine. 2011;6:1117-27.
 11. Shah M, Fawcett D, Sharma S, Tripathy SK, Poinern GEJ. Green Synthesis of Metallic Nanoparticles via Biological Entities. Materials. 2015;8:7278-308.
 12. Guangquan L, Dan H, Yongqing Q, Buyuan G, Song G, Yan C. Fungus mediated green synthesis of silver nanoparticles using *Aspergillus terreus*. Int. J. Mol. Sci. 2012;13:466-76.
 13. Shanmugavadivu M, Kuppusamy S, Ranjithkumar R. Synthesis of pomegranate peel extract mediated silver nanoparticles and its antibacterial activity. Am. J. Adv. Drug Deliv. 2014;2(2):174-82.
 14. Sastry M, Ahmad A, Khan MI, Kumar R. Biosynthesis of metal nanoparticles using fungi and actinomycete. Curr. Sci. 2003;85:162-70.
 15. Lengke M, Southam G. Bioaccumulation of gold by sulphate-reducing bacteria cultured in the presence of gold (I)-thiosulfate complex. Acta. 2006;70:3646-61.
 16. Kuber C, Souza SF. Extracellular biosynthesis of silver nanoparticles using the fungus *Aspergillus fumigatus*. Colloids Surf B. 2006;47:160-4.
 17. Poinern GEJ, Shah M, Chapman P, Fawcett D. Green biosynthesis of silver nanocubes using the leaf extracts from *Eucalyptus macrocarpa*. Nano Bulletin. 2013;2(130101):1-5.
 18. Lee SW, Mao C, Flynn C, Belcher AM. Ordering of quantum dots using genetically engineered viruses. Science. 2002;296:892-5.
 19. Gericke M, Pinches A. Biological synthesis of metal nanoparticles. Hydrometallurgy. 2006;83:132-40.
 20. Mohanpuria P, Rana NK, Yadav SK. Biosynthesis of nanoparticles: technological concepts and future applications. J. Nanopart. Res. 2008;10:507-17.
 21. Kumar V, Yadav SK. Plant-Mediated Synthesis of Silver and Gold Nanoparticles and Their Applications. Journal of Chemical Technology and Biotechnology. 2009;84(2):151-7.
 22. Malik P, Shankar R, Malik V, Sharma N, Mukherjee TK. Green Chemistry Based Benign Routes for Nanoparticle Synthesis. Journal of Nanoparticles. 2014; Article ID 302429, 14 pages.
 23. Rai M, Yadav A, Gade A. Silver nanoparticles as a new generation of antimicrobials. Biotechnol. Adv. 2009;27:76-83.
 24. Jorgensen JH, Turnidge JD. Susceptibility test methods: dilution and disk diffusion methods. In Murray PR, Baron EJ et al (ed) Manual of clinical microbiology, 9th edn. ASM Press, Washington DC. 2007;1152-72.
 25. Chandan-Singh ML, Vinect-Sharma KR. A green biogenic approach for synthesis of gold and silver nanoparticles using *Zingiber officinale*. Digest Journal of Nanomaterials and Biostructures. 2011;6(2):535-42.
 26. Zahir AA, Bagavan A, Kamaraj C, Elango G, Rahuman AA. Efficacy of Plant-Mediated Synthesized Silver Nanoparticles against *Sitophilus oryzae*. Journal of Biopesticides. 2012;288 (Suppl-5):95-102.
 27. Ahmad N, Sharma S, Alam MK, Singh VN, Shamsi SF, Mehta BR, Fatma A. Rapid Synthesis of Silver Nanoparticles Using Dried Medicinal Plant of Basil. Colloids and Surfaces B: Biointerfaces. 2010;81(1):81-6.

Cite this article as: Shah M, Poinern GEJ, Fawcett D. Biogenic synthesis of silver nanoparticles via indigenous *Anigozanthos manglesii*, (red and green kangaroo paw) leaf extract and its potential antibacterial activity. Int J Res Med Sci 2016;4: 3427-32.